ELSEVIER

Thermochimica Acta 362 (2000) 99–105

thermochimica acta

www.elsevier.com/locate/tca

Influence of γ-irradiation and Dy_2O_3 on the decomposition of barium oxalate: A thermogravimetric study

H. Nayak, D. Bhatta*

Department of Chemistry, Utkal University, Bhubaneswar, Orissa 751004, India

Received 21 September 1999; received in revised form 24 April 2000; accepted 22 June 2000

Abstract

Effect of γ-irradiation (4.0 MGy) and the presence of Dy_2O_3 (10 mol%) on the decomposition of anhydrous barium oxalate has been investigated by the rising temperature technique. It is evident from the data that in all the materials, decomposition occurs through (i) a slow reaction stage and (ii) a fast stage followed by a decay period. The loss of 'CO' from the oxalate is governed by a two-dimensional phase boundary reaction with cylindrical geometry, the power law of the reaction order, 0.5, in the irradiated salt and three-dimensional nuclei growth in case of mixture. The data were well explained by the contracting area (R_2) model indicating that irradiation as well as mixing enhanced the rate of reaction and decreased the energy of activation, the effect being more prominent in the latter case.

Keywords: Kinetics; Decomposition; γ-Irradiation; Dy_2O_3; Barium oxalate

1. Introduction

The kinetics of decomposition of oxysalts have been extensively studied by Dollimore and Griffith [1]. It has been reported that barium oxalate monohydrate is stable up to 76°C, beyond which the loss of water molecules takes place [2] and the anhydrous salt decomposes at 340°C [3,4]. Verdonk et al. [5] carried out the reaction in the presence of dry nitrogen and suggested that part of the evolved gas disproportionated leaving carbon.

The effect of γ-irradiation and mixing with other compounds on the thermal decomposition of alkali and alkali-earth metal oxalates have been studied gasometrically by many workers [6,7] and it is indicated that both the treatments facilitate the reaction and decrease the energy of activation. The present work has been carried out using the rising temperature technique. This is different from the isothermal study, as in this process some of the defects and dislocations generated by irradiation and mixing are annealed prior to decomposition, hence their effect on the process is diminished.

2. Experimental

Barium oxalate was prepared by precipitation from oxalic acid (AR grade) and barium nitrate (AR grade) in a dilute aqueous solution and the crystals were dehydrated in vacuum at 493 K to a constant weight. Purity (99.9%) of the sample was checked by estimating barium by flame photometrically and oxalate by chemical analysis.

The anhydrous sample, sealed in vacuum in glass ampoules, was exposed to ^{60}Co γ-ray (4.0 MGy) at a dose rate of 0.108×10^{-2} MGy h^{-1} as determined by

* Corresponding author. Tel.: +91-674-582186.

0040-6031/00/$ – see front matter
PII: S0040-6031(00)00585-2

Fricke ferrous sulphate dosimeter, G $(Fe^{3+}) = 15.5$, and the crystals were stored in a desiccator before use.

The physical mixture (300-mesh size) of barium oxalate and Dy_2O_3 (10.0 mol%) was prepared from their corresponding weights and grinding together in an agate mortar.

Decomposition study on normal and irradiated BaC_2O_4 as well as the $(BaC_2O_4 + Dy_2O_3)$ mixture was undertaken between 713 and 803 K by a dynamic method using TG [Shimadzu Model DTG 50] at a heating rate of $10^{\circ}C\,min^{-1}$ in an oxygen atmosphere.

3. Result and discussion

Irradiation imparts a brown colour to the crystals which gradually disappears on heating and may be attributed to colour centres. The following sequence of reaction steps (in air) cover the TG weight losses satisfactorily in the temperature range:

$$BaC_2O_4(s) \rightarrow BaCO_3 + CO(g); \quad 330-470-550^{\circ}C \tag{1}$$

$$2CO(g) \rightarrow C(S) + CO_2(g); \quad 470-550^{\circ}C \tag{2}$$

Between 330 and 470°C, the reaction proceeds at a detectable rate, but step (2), although thermodynamically favoured at this temperature range, is kinetically inhibited [8]. A suitable range, 440–530°C was chosen which is observable due to more favourable condition for nuclei growth.

The thermograms of unirradiated and irradiated crystals as well as the mixture are redrawn as the fraction decomposed, α versus the temperature, T (TG) curves, as well as the rate of change of α, i.e. $d\alpha/dT$ versus T and the peak temperatures of different DTG are noted.

Decomposition data (Table 1) on unirradiated and irradiated salts as well as the mixture are shown in Fig. 1, suggesting that the reaction occurs through slow and fast stages followed by a decay period. The important stage between 440 and 550°C, during which maximum decomposition takes place, occurs at a lower temperature in case of an irradiated crystal.

Table 1
Decomposition temperatures for dissociation of BaC_2O_4 to $BaCO_3$ determined at a heating rate of $10^{\circ}C\,min^{-1}$

Sample[a]	Temperature[b] (°C)	
	T_i	T_f
BO1	490	530
BO2	450	520
BO3	440	490

[a]BO1, Unirradiated BaC_2O_4; BO2, $BaC_2O_4 + Dy_2O_3$; BO3, irradiated BaC_2O_4.

[b]T_i and T_f refer to the inception and final temperature determined from TG.

4. Determination of order of reaction

The order of a reaction was determined from the DTG plot as suggested by Horowitz and Metzger [9]

$$C_s = n^{1/(1-n)}$$

where n is the order of reaction, C_s the weight fraction present at the temperature T_s corresponds to the DTG peak. Data on all categories of materials are incorpo-

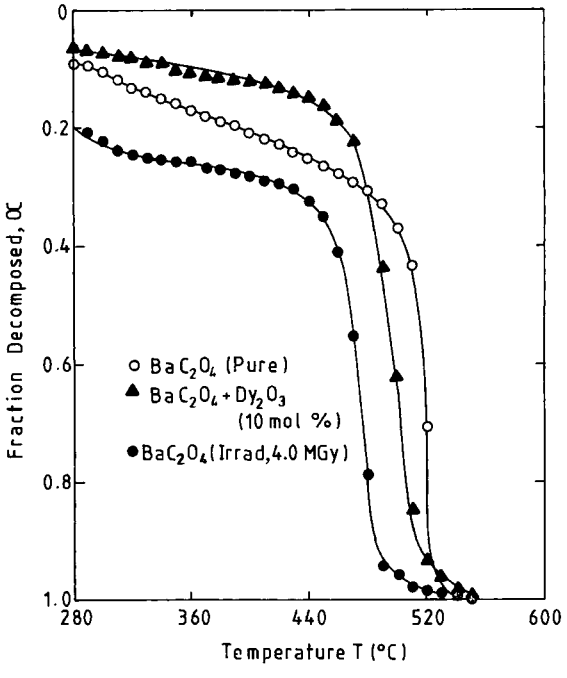

Fig. 1. TG curves of the thermal decomposition of BaC_2O_4 to $BaCO_3$ for unirradiated, and irradiated crystals and BaC_2O_4+ Dy_2O_3 mixture.

Table 2
Values of the order of reaction and $1-\alpha$, for $(d\alpha/dT)_{max}$

n[a]	0.10	0.30	0.50	0.70	1.00	1.50	2.00	3.00	4.00	5.00
$1-\alpha$	0.008	0.18	0.25	0.30	0.37	0.44	0.50	0.58	0.63	0.67

[a]Order of reaction.

rated in Table 2. A master curve is plotted between C_s and n and the latter is obtained for determined values of C_s as reported earlier [10].

5. Interpretation of kinetics data

Kinetic parameters for the important stage of decomposition, 440–530°C are determined from the Coat–Redfern equation

$$\log\frac{g(\alpha)}{T^2} = \log\frac{AR}{\beta E} - \frac{E}{2.303RT} \quad (3)$$

where A is the pre-exponential factor, β the heating rate, E the energy of activation, R the Universal gas constant and T the absolute temperature.log $[g(\alpha)/T^2]$ is calculated for each possible rate controlling mechanism using models P_1, A_2, A_3, A_4, D_3 and R_2 (Table 3) and plotted against $1/T$, one such plot for the power law (P_1) is represented in Fig. 2.

The value of $g(\alpha)$ with the highest correlation coefficient of linear regression analysis (r) gives the idea regarding the best fit mechanism which is obtained by fitting the data on log $g(\alpha)/T^2$ and $1/T$ to Eq. (3). Adopting such an idea, values of $g(\alpha)$ are chosen out of Figs. 3–5 for different samples.

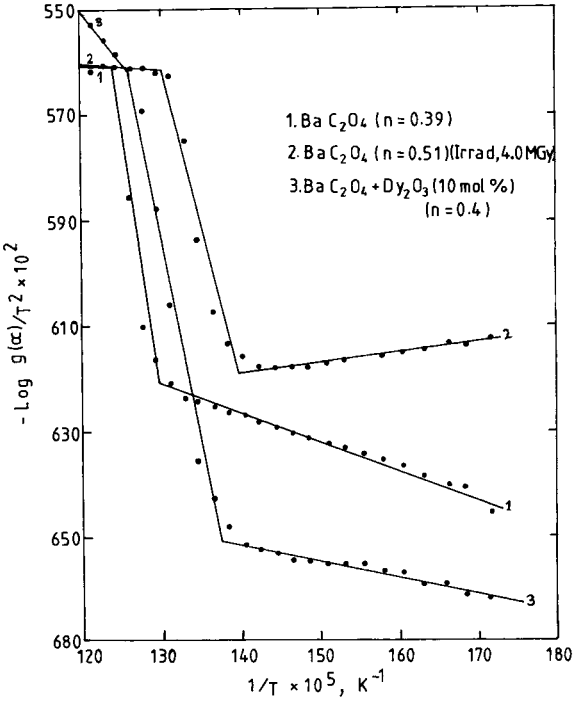

Fig. 2. Variation of log $g(\alpha)/T^2$ vs. $1/T$ for decomposition of unirradiated and irradiated BaC_2O_4 and $BaC_2O_4 + Dy_2O_3$ mixture using power law.

Table 3
Different kinetic models of the decomposition of BaC_2O_4

Rate determining mechanism	Symbol	$g(\alpha)$
Avrami–Erofeev nuclei growth		
two-dimensional	A_2	$[-\ln(1-\alpha)]^{1/2}$
three-dimensional	A_3	$[-\ln(1-\alpha)]^{1/3}$
four-dimensional	A_4	$[-\ln(1-\alpha)]^{1/4}$
Diffusion mechanism: three-dimensional	D_3	$[-\ln(1-\alpha)^{1/3}]^2$
Power law	P_1	$1-(1-\alpha)^{1/2}$ n=0.51
Phase boundary movement, two-dimensional (cylindrical symmetry)	R_2	$1-(1-\alpha)^{1/2}$

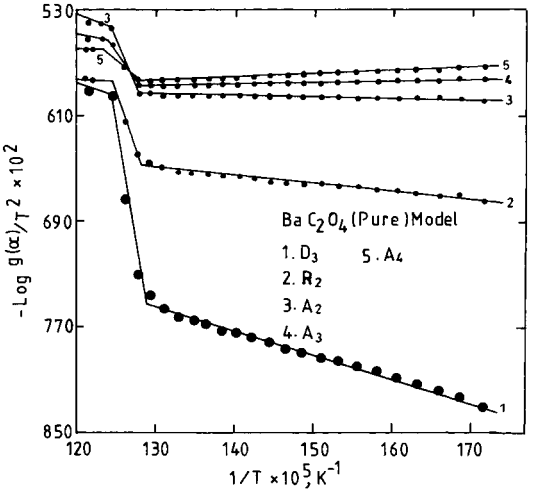

Fig. 3. Variation of $\log g(\alpha)/T^2$ vs. $1/T$ for decomposition of BaC_2O_4 using D_3, R_2, A_2, A_3 and A_4 models.

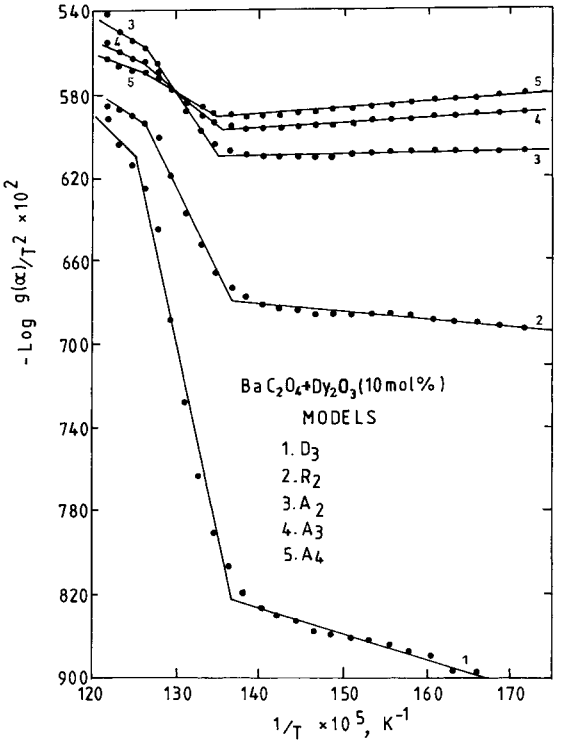

Fig. 4. Variation of $\log g(\alpha)/T^2$ vs. $1/T$ for Decomposition of $BaC_2O_4 + Dy_2O_3$ (10 mol%) mixture using various models.

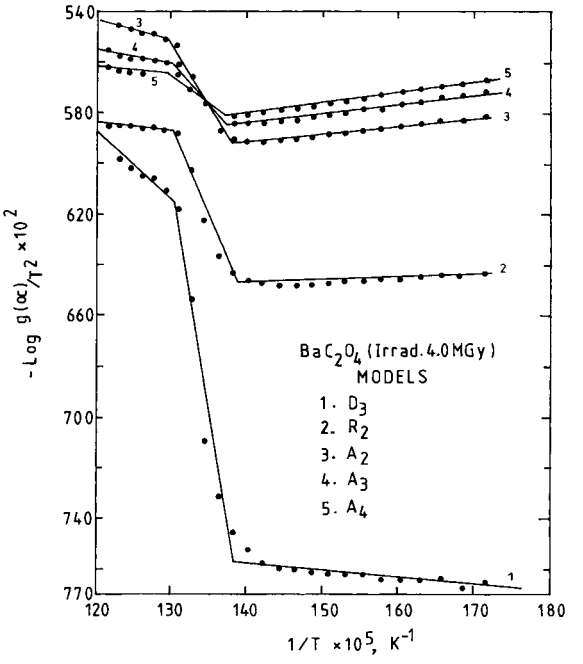

Fig. 5. Variation of $\log g(\alpha)/T^2$ vs. $1/T$ for decomposition of irradiated BaC_2O_4 (4.0 MGy) using various models.

The values of activation energy E and frequency factor A are calculated from the slopes and intercepts of plots of $\log g(\alpha)/T^2$ versus $1/T$ for each sample, thus indicating the different stages of decomposition: slow, acceleratory and decay. The plausible mechanism and corresponding kinetic parameters as well as correlation coefficients for different materials are incorporated in Table 4.

The best fit mechanism in each case with the highest r value together with energy of activation E and frequency factor A are represented in Table 5 and Fig. 6.

6. Analysis of the kinetics data

It is evident from the data (Table 1) that inception as well as final temperatures, calculated from TG curve are decreased by irradiation as well as by the admixture suggesting that these treatments favour the process. Considering the data in the light of R_2 model, it is suggested that above treatments facilitate the reaction rate (Table 4), the effect being higher in the case of irradiation.

Table 4
Controlling process and kinetic parameters for decomposition of anhydrous barium oxalate in air at a heating rate of 10°C min^{-1}

Sample	Mechanism $g(\alpha)$	$E(\pm5)$ (kJ mol^{-1})	$\log(As^{-1})(\pm2)$	r^a	K^b (±0.5) (s^{-1})
BO1	P_1	145.12	8.92	0.9789	0.1303
	A_2	154.88	9.79	0.9887	0.2097
	A_3	74.97	4.17	0.9876	0.1272
	A_4	63.02	3.29	0.9899	0.1076
	D_3	435.70	27.73	0.9567	0.0196
	R_2	165.03	10.03	0.9989	0.0758
BO2	P_1	168.62	10.81	0.9746	0.2614
	A_2	91.12	5.42	0.9991	0.1833
	A_3	57.43	2.95	0.9988	0.1161
	A_4	87.99	5.18	0.9893	1.1701
	D_3	314.34	19.84	0.9835	0.0399
	R_2	144.36	8.74	0.9719	0.0969
BO3	P_1	141.9	9.48	0.9939	0.7756
	A_2	96.1	6.26	0.9763	0.5849
	A_3	62.5	3.71	0.9796	0.3061
	A_4	41.98	2.09	0.9892	0.1793
	D_3	650.06	23.54	0.9733	0.7735
	R_2	150.47	9.84	0.9888	0.4716

[a] Correlation coefficient.
[b] Rate constant determined at 500°C.

An interesting phenomenon observed is that though irradiation increase the rate of decomposition remarkably there is not much decrease in the energy of activation.

By discussing the data in the light of theories of different best fit kinetic models; R_2, A_2 and P_1 ($n = 0.51$), the rate of reaction and the activation energy are calculated which follows the order: irradiated material > mixture > unirradiated salt, and unirradiated salt > irradiatedcrystal > mixture, respectively.

Applicability of contracting area kinetics to unirradiated crystal suggests that the initial nucleation occurs rapidly over the entire surface for a single cylinder of reactant and, thereafter, the interface established progresses in the direction of the centre of the crystal. The reaction is deceleratory throughout as its interface progressively decreases. The mechanism is governed by the conversion integral:

$$g(\alpha) = 1 - (1 - \alpha)^{1/n} \quad (n = 2) \tag{4}$$

where n is the number of dimensions in which the interface advances, the nucleation having taken place on all faces. When nucleation is restricted to specific crystallographic surfaces, the advance of interfaces into the bulk of the reactant particles takes place from those surfaces.

Admixture Dy_2O_3 changes the decomposition mechanism and the data on the sigmoidal region satisfactorily fit to Avrami–Erofeev relationship

$$g(\alpha) = [-\ln(1 - \alpha)]^{1/2} \quad (n = 2) \tag{5}$$

Table 5
Kinetic parameters derived for best-fit rate controlling processed for the dynamic decomposition of BaC_2O_4 to $BaCO_3$ using the Coat–Redfern method

Sample	$g(\alpha)$	$E(\pm5)$ (kJ mol^{-1})	$\log(As^{-1})(\pm2)$	r	K (±0.05)$\times10^2$ (s^{-1})
BO1	R_2	165.03	10.03	0.9989	7.58
BO2	A_2	91.12	5.42	0.9991	18.33
BO3	P_1	141.9	9.48	0.9939	77.56

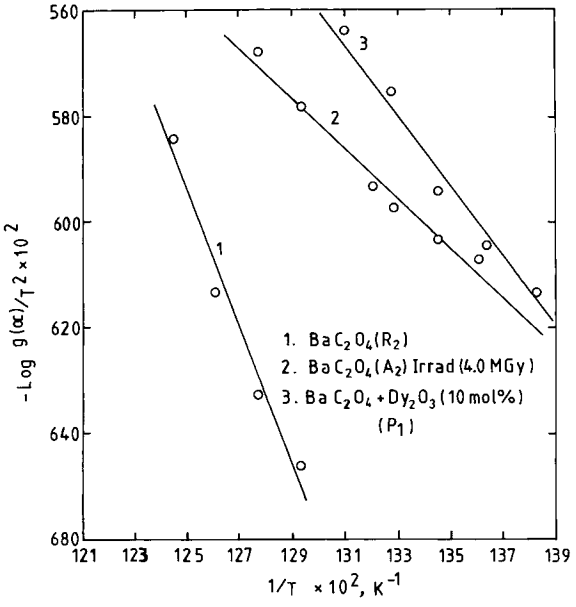

Fig. 6. Variation of $\log g(\alpha)/T^2$ vs. $1/T$ for decomposition of unirradiated and irradiated BaC_2O_4 and ($BaC_2O_4 + Dy_2O_3$) mixture using best fit models R_2, A_2 and P_1 at the temperature range 440–530°C.

suggesting that there is an instantaneous and random nucleation [11,12], followed by a two-dimensional growth of nuclei during the decomposition process. The value of $n = 2$ in Eq. (5) suggests that the decomposition site is a surface of disc, or cylinder and instantaneous nucleation results in complete consumption of surfaces, thereby eliminating the sites of nucleation and diminution of n. The continued inward advance of the reaction interface at higher α results in a situation comparable with contracting areas reaction.

Considering the data in the light of power law

$$g(\alpha) = \frac{1-(1-\alpha)^{1-n}}{1-n} \quad (n = 0.51) \tag{6}$$

it is suggested that there is random nucleation followed by constant advancement of the interface.

7. Role of irradiation

Upon exposure of barium oxalate to γ-rays, excitation, ionisation followed by rupture of the chemical bonds of the anion takes place as the γ-ray energy, $E_\gamma >$ C–C (3.6 eV), C–O (3.7 eV), C=O (7.7 eV) bond energies. In addition to damaged entities, trapped electrons (e^-) and holes (h^+), radicals and ions are also generated which constitute decomposition nuclei themselves and may be termed as irradiation nuclei, n_i. Due to generation of defects and dislocations, additional nucleation centres are created in the lattice which fracture the crystal, forming new potential centres and the reaction thereafter follows a fast step, consequently enhancing the reaction rate and decreasing the energy of activation.

8. Effect of admixture

The catalytic activity of Dy_2O_3 on the decomposition process may be explained in the light of electron transfer mechanism [13]:

$$C_2O_4^{2-} + Ba^{2+} \rightarrow C_2O_4^{-} + Ba^{2+}(e^- \text{ absorbed}) \tag{7}$$

$$Ba^{2+}(e^- \text{ adsorbed}) \rightarrow Ba^{2+} + e^- \text{ (to solid catalyst)} \tag{8}$$

The oxides of the rare earths are strongly basic [14] in nature and donate electrons there by regenerating $C_2O_4^{2-}$ from $C_2O_4^{-}$ ion, thus increasing the number of positive holes in the lattice and the following reaction may be envisaged:

$$C_2O_4^{2-} \rightarrow [OCOCO_2]^{2-} \rightarrow CO_3^{2-} + CO \rightarrow O^{2-} + CO_2 + CO \tag{9}$$

Dy_2O_3 being a p-type semiconducter [15] is more conducting in the oxygen atmosphere [16] and facilitates the process by accepting electrons from the adsorbed Ba^{2+} ion in the rate determining step (6), thereby increasing the rate of the reaction. It has been reported [17] that catalytic activity of metal oxides on the thermal decomposition of oxalates is enhanced as the ionic radii of the metal ion is decreased. Dy^{3+} with small atomic size (hence less basic) is capable of accepting the adsorbed electron more favourably from the Ba^{2+} ion. Hence, the catalyst decreases the free energy of activation of both the reactant and product, consequently favouring the nucleation and nucleus growth and resulting in a faster decomposition.

Acknowledgements

H. Nayak thanks CSIR, New Delhi, for financial assistance as a research fellowship.

References

[1] D. Dollimore, D.L. Griffith, J. Therm. Anal. 2 (1970) 229.
[2] J.C. Mutin, G. Watelle-Marion, C.R. Acad. Sci. Ser. C 266 (1968) 315.
[3] G. Brunhs, Z. Anorg. Allg. (1916) 194.
[4] G. Brunhs, Chem. Zentralbl. 11 (1916) 454.
[5] S. Bose, K.K. Sahu, D. Bhatta, J. Radioanal, Nucl. Chem. (Articles) 181 (1994) 441.
[6] S. Bose, K.K. Sahu, D. Bhatta, J. Therm. Anal. 44 (1995) 1131.
[7] S. Bose, K.K. Sahu, D. Bhatta, Thermochim. Acta 268 (1995) 175.
[8] A.H. Verdonk, A. Broersma, Thermochim. Acta 6 (1973) 95.
[9] K.G. Nair, V.V. Sreerajan, V.S.V. Nayar, C.G.R. Nair, Thermochim. Acta. 39 (1980) 253.
[10] P.M. Madhusudanan, P.N.K. Nambisan, C.G.R. Nair, Thermochim. Acta. 9 (1974) 149.
[11] J. Jach, in: Reactivity of Solid, Elsevier, Amsterdam, 1961, 334 pp.
[12] K.C. Wieczorck, J. Paulik, F. Paulik, Thermochim. Acta 38 (1980) 157.
[13] H. Bamford, C.F.H. Tipper (Eds.), Comprehensive Chemical Kinetics, vol. 22, Reaction in Solid State, Elsevier, Amsterdam, 1980, 219 pp.
[14] A.M. Maitra, J. Therm. Anal. 36 (1990) 657.
[15] F. Jasim, K.R. Idan, J. Therm. Anal. 21 (1981) 249.
[16] D. Bhatta, S. Mishra, K.K. Sahu, J. Therm. Anal. 39 (1993) 275.
[17] D.A. Templeton, C.H. Dauben, J. Am. Chem. Soc. 76 (1954) 5237.